Thermochimica Acta 517 (2011) 1–8

Contents lists available at ScienceDirect

Thermochimica Acta

journal homepage: www.elsevier.com/locate/tca

Thermodynamic assessment of the In–Ir system in the In rich part

Colette Servant [a], Mohamed Idbenali [b,*]

[a] Laboratoire de Physicochimie de l'Etat Solide, ICMMO, Université de Paris-Sud, 91405 Orsay Cedex, France
[b] Laboratoire de Thermodynamique Métallurgique et Rhéologie des Matériaux, Université Ibn Zohr, B.P. 496, Dcheira, Agadir, Morocco

ARTICLE INFO

Article history:
Received 4 August 2010
Received in revised form
13 December 2010
Accepted 22 December 2010
Available online 13 January 2011

Keywords:
In–Ir system
CALPHAD method
Thermodynamic assessment
Phase diagram

ABSTRACT

Optimization by the CALPHAD method of the thermodynamic parameters of the In–Ir system has been carried out using the experimental phase diagram data and thermodynamic properties. The numerous experimental data of the liquid phase determined in the $0 < x(\mathrm{Ir}) < 0.35$ composition range by two authors are coherent and associated with the scarce enthalpies of formation of the two intermetallic compounds allowed to optimize a set of coherent thermodynamic parameters in order to calculate the phase diagram in the In rich part. In the $0.40 < x(\mathrm{Ir}) \leq 1$ composition range, the phase diagram seems more complex than the schematic part extrapolated at high temperature and the agreement between the calculated diagram and this extrapolated experimental part is not satisfactory. Further experimental investigations are needed to improve the calculation in this composition range, but which are difficult because hampered by different phenomena.

1. Introduction

The last few years, the binary indium compounds (such as InP, InAs, and InSb) have been largely investigated due to their important technological properties. Belonging to the A^{III}–B^{V} semiconductors, they have applications in electronic and optoelectronic devices. In order to found out which elements are stable in contact with the III–V semi-conductor, ternary M–III–V (with M = metal) phase diagrams such as In–As–Ir, In–Sb–Ir are necessary to be assessed. Yet before, the low-order systems must be mandatory determined. The In–Ir binary system has not been genuinely studied experimentally [1–5]. The phase diagram available in the literature is not complete [6–8]. The In rich part, up to $x(\mathrm{Ir}) = 0.5$, has been reviewed since 1998 [9–12]. Two intermetallic compounds have been identified as In_3Ir and In_2Ir. Their crystal structures, determined by refinement of X-ray diffraction diagrams are reliable. In_2Ir has two crystallographic independent iridium networks with stronger interaction within and weaker one between the networks. It is a good metallic conductor and Pauli paramagnet [13]. Thermodynamic properties have been determined in particular for the liquid phase [11,12]. As regards the two intermetallic compounds, only the enthalpy of formation of In_3Ir measured by high temperature drop calorimetry [14] is reliable. Because of the large differences in the melting temperatures of In (429 K) and Ir (2723 K), the evaporation of In must be accurately controlled and taken into account during the experimental determinations. In addition, the sluggishness of the equilibration may hamper these experiments. As no thermodynamic assessment was performed before, the aim of the present work was to optimize a set of consistent thermodynamic parameters of the different phases of the In–Ir system by the CALPHAD method [15] which will serve later to assess ternary systems M–In–Ir.

2. Experimental data

2.1. Phase diagram data

The shape of the phase diagram has first been drawn by Moffat [6] in comparison to the one of the Co–In system which displays two definite compounds $CoIn_3$ and $CoIn_2$ melting incongruently and a miscibility gap with a very high critical temperature. The liquidus part $Liq/Liq + In_3Ir$ was determined using differential calorimetry by Schubert et al. [1,2] between 600 and 1250 K, as well as the existence of two intermetallic compounds In_3Ir and In_2Ir, Table 1, reported later by Ellner and Bhan [5]. Schubert et al. [1,2] also determined a eutectic reaction $Liq \leftrightarrow In\ tetragonal\_A6 + In_3Ir$ and two peritectic reactions $Liq + In_2Ir \leftrightarrow In_3Ir$ and $Liq + (Ir) \leftrightarrow In_2Ir$ in the $0 \leq x(\mathrm{Ir}) < 0.5$ composition range. The solubility of iridium in indium in the temperature range 600–1240 K has been measured by Dieva [4]. Two data of the $Liq/Liq + In_3Ir$ liquidus part were assessed by Anres et al. [11] by calorimetric measurements in good agreement with the data of Schubert [1,2], and three data of the $Liq/Liq + In_2Ir$ liquidus part. By differential thermal analysis Anres et al. [11] measured the temperatures of the eutectic (about 1258 K) and peritectic

* Corresponding author. Tel.: +33 1 69157021; fax: +33 1 69157833.
E-mail addresses: coletteservant@orange.fr (C. Servant), idbenalimohamed@yahoo.fr (M. Idbenali).

0040-6031/$ – see front matter © 2011 Elsevier B.V. All rights reserved.
doi:10.1016/j.tca.2010.12.019

Table 1
Symbols and crystal structures of the solid phases in the In–Ir alloys.

Diagram symbol	Composition at % Ir	Symbol use in Thermo-Calc data file	Pearson symbol [24]	Space group	Strukturbericht designation	Prototype
In	0	Tetragonal_A6	*tI2*	*I4/mmm*	A6	In
In_3Ir_HT	25	In_3Ir_HT	*tP16*	$P4_2/mnm$		$FeGa_3$
In_3Ir_LT	25	In_3Ir_LT	*oP16*	*Pnma*		$CrFe_3$
In_2Ir	33.33	In_2Ir	*oF48*	*Fddd*		$CuMg_2$
$In_{54}Ir_{46}$	46	Metastable				
Ir	100	FCC_A1	*cF4*	$Fm\bar{3}m$	A1	Cu

(about 1463 K) reactions and pointed out the difficulty to reach the (solid + liquid) equilibrium. A change of structure LT ↔ HT was noticed at 625 K for In_3Ir.

New experimental phase diagram data assessed by Flandorfer et al. [12] based on X-ray diffraction, Electron Probe Microscopy Analysis (EPMA) and Differential Thermal Analysis (DTA) was published in 2002. A metastable phase $In_{54}Ir_{46}$ was found. A small homogeneity range was determined for the In_2Ir and In_3Ir phases. For this latter phase, a metatectic reaction was suggested as In_3Ir_HT <-> Liq + In_3Ir_LT, at temperatures below 625 K [11] or 620 ± 3K [12], as well as a peritectoïd reaction In_2Ir + In_3Ir_HT <-> In_3Ir_LT at 636 ± 3K [12]. The temperatures of all the invariant reactions were indicated for $0 \leq x$ (Ir) ≤ 0.5. A (Ir) fcc solid solution with a very small amount of In (0.01%) was also mentioned. The new phase diagram drawn by [12] with the above more recent experimental data is shown in Fig. 1. Beyond x(Ir) >0.4, the liquidus is unknown and drawn with a dashed line as well as the two-phase domain (Liq + (Ir)).

2.2. Thermodynamic data

The integral and partial molar enthalpies of mixing of the liquid phase have been first determined by Anres et al. [11] using the direct drop method with a high temperature calorimeter in the temperature range 1175-1589 K for $0 < x$(Ir) < 0.26, and at 1154 K and for $0 < x$(Ir) ≤ 0.02. In and Ir purities were 99.99 wt %. The errors in the enthalpies of mixing and in the molar fraction x(Ir) were, respectively, assessed at about ± 4% and less than ± 1%. They indicated that the enthalpy of mixing of the liquid phase seems not be temperature dependent within the experimental error in the temperature and molar fraction ranges studied. They found that at 1154 K the limiting partial molar enthalpy of mixing of hypothetically supercooled liquid iridium in liquid indium is equal to −50 ± 2 kJ/mol.

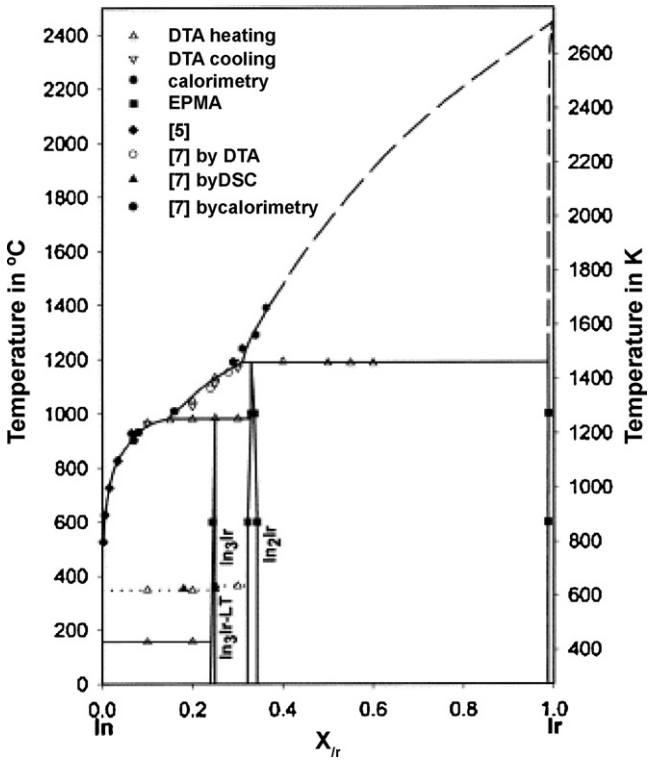

Fig. 1. The In–Ir phase diagram drawn by Flandorfer et al. [12].

Later on, Flandorfer et al. [12] determined the integral enthalpies of mixing of the liquid phase by means of a high temperature drop calorimeter in the 1463–1663 K temperature range. They claimed that the limiting partial enthalpy of mixing of liquid Ir in liquid In (about −50 kJ/mol) does not depend significantly on temperature, while the integral enthalpy of mixing of the liquid phase, which reaches −12 to −15 kJ/mol, depends on temperature. A liquid miscibility gap, as earlier suggested in the literature [6], which would need that the Gibbs energy of mixing of the liquid phase becomes positive, was excluded. On the other hand, authors of [11] indicated the possibility of the existence of a liquid–liquid miscibility gap because the extremum of the curve $\Delta_{mix}H^0_m = f(x_{(Ir)})$ is one of the less exothermic ones for the alloy series consisting of a group VIII transition metal and a sp metal (Ga or In essentially) and moreover of the great similarity observed between the Co–In and In–Ir systems.

The theoretical values predicted by the Miedema's model were 0 J/mol for the integral enthalpy of mixing of the liquid phase for x(Ir) = 0.5 and −1 J/mol for the limiting partial molar enthalpy of dissolution of Ir in In and In in Ir [16]. Molar enthalpies of formation of the intermetallic compounds have been determined by [11] on the basis of the plots of the integral enthalpies of mixing of the liquid phase versus x(Ir) drawn at 1175 K for In_3Ir, and at 1204, 1282 and 1359 K for In_2Ir, according to the respective reactions:

$$3In(liq) + Ir(liq) \rightarrow In_3Ir\,(sol)$$
$$2In(liq) + Ir(liq) \rightarrow In_2Ir\,(sol).$$

The values were −9 ± 2 kJ/mol and −14 ± 2 kJ/mol, respectively.

Another measurement of the molar enthalpy of formation of In_3Ir was made in 2002 by Meschel and Kleppa [14] in the case of the determination of standard enthalpies of formation of some transition metal–indium compounds by high temperature direct synthesis calorimetry. For In_3Ir_HT the average value of six or seven consecutive measurements with the appropriate standard deviation obtained was −23.8 ± 2.4 kJ/mol of atoms at 1273 ± 2 K. The pattern of In_3Ir matched well with the generated pattern by X-ray diffraction. No unreacted metals or secondary phases were detected [14]. So, this experimental procedure is more reliable that the extrapolation method used by Anres et al. [11] (data derived on the basis of the precipitation of solid compounds from the liquid marked by kinks on the curve of the integral enthalpy of mixing of the liquid phase versus x(Ir)) which can have an important uncertainty.

Let us remind that the theoretical values predicted by the semi-empirical model of Miedema and co-workers [16] at

298.15 K were, respectively, −10 kJ and −13 kJ/mol of atoms for In_3Ir and In_2Ir.

Anres et al. [11] also determined the molar heat capacities between 423 and 763 K for three alloys of x(Ir) composition equal to 0.186, 0.25 and 0.33.

3. Thermodynamic models

3.1. Pure elements

The Gibbs energy function (298.15 K) for the element i (i = In, Ir) in the ϕ phase (ϕ = liquid, tetragonal_A6 or FCC_A1) is described by an equation of the following form:

$$G_i^{\phi}(T) = a + bT + cT\ln T + dT^2 + eT^3 + fT^7 + gT^{-1} + hT^{-9} \quad (1)$$

In this paper, the Gibbs energy functions are taken from the SGTE compilation of Dinsdale [17]. These functions are, respectively, valid up to T = 3800 K and 4000 K for In and Ir.

3.2. Solution phases

The Gibbs energy of one mole of formula unit is expressed as the sum of three terms:

$$G^{liq} - H^{SER} = {}^{ref}G^{liq} + {}^{id}G^{liq} + {}^{ex}G^{liq} \quad (2)$$

$${}^{ref}G_{liq} = x_{In}\left[{}^{0}G_{In}^{liq} - H_{In}^{SER}\right] + x_{Ir}\left[{}^{0}G_{Ir}^{liq} - H_{Ir}^{SER}\right] \quad (3)$$

where H_i^{SER} (298.15K) is the molar enthalpy of the i element at 298.15 K in its Standard Element Reference (SER) state, tetragonal_A6 for In and FCC_A1 for Ir.

$${}^{id}G_{liq} = RT(y_{In}\ln y_{In} + y_{Ir}\ln y_{Ir}) \quad (4)$$

where R is the ideal gas constant; T is the temperature, in Kelvin; x_{In} and x_{Ir} are the mole fraction of the elements In and Ir, respectively.

The ${}^{ex}G^{liq}$ energy part in Eq. (2) is given by the Redlich–Kister polynomial [18]

$${}^{ex}G_{liq} = y_i y_j \sum_{\lambda=0}^{\lambda} {}^{\lambda}L_{i,j}^{Liq}(y_i - y_j)^{\lambda} \quad (5)$$

with i and j are indices which correspond to the two species In and Ir.

The binary interaction parameters of the ${}^{\lambda}L_{i,j}^{Liq}$ type, assessed in the present work, were temperature dependent as follows:

$${}^{\lambda}L_{i,j}^{Liq} = a_{\lambda} + b_{\lambda}T \quad (6)$$

a_{λ} and b_{λ} are the coefficients to be optimized.

The tetragonal_A6 and FCC_A1 phases were, respectively, modelled as pure In because of the unknown and certainly very low solubility of Ir in In and as a solution phase (Ir).

3.3. Stoichiometric compounds and intermediate phases

In_3Ir and In_2Ir were first considered as stoichiometric compounds, their Gibbs energy noted as ${}^{0}G_{ApBq}$ was expressed as follows:

$${}^{0}G_{ApBq} = \frac{p}{p+q}{}^{0}G_A + \frac{q}{p+q}{}^{0}G_B + a + bT \quad (7)$$

where ${}^{0}G_A$ and ${}^{0}G_B$ are the Gibbs energy of the pure elements In and Ir, respectively; a and b are parameters to be determined.

As the In_3Ir and In_2Ir intermetallic compounds have an experimental small homogeneity range [12], in a second step, they were treated by a two-sublattice model. The experimental extension of In_3Ir is towards the In rich part (substoichiometric compound) while the one of In_2Ir is from one part to another of the stoichiometric composition, so the respective modelling were as follows: $(In)_{0.75}(In,Ir\%)_{0.25}$ and $(In\%,Ir)_{0.6667}(In,Ir\%)_{0.3333}$. The symbol % denotes the major component in the considered sublattice.

The Gibbs energy function per mole (m) of the formula unit $(In)_{0.75}(In,Ir\%)_{0.25}$ is the following:

$$G^{0.75In0.25Ir} - H_{0.75In0.25Ir}^{SER} = y_{In}^1 y_{In}^2\,{}^{0}G^{In:In} + y_{In}^1 y_{Ir}^2\,{}^{0}G^{In:Ir} + RT\left[0.75y_{In}^1\ln y_{In}^1 + 0.25(y_{In}^2\ln y_{In}^2 + y_{Ir}^2\ln y_{Ir}^2)\right] + {}^{xs}G_m \quad (8)$$

$$H_{In0.75Ir0.25}^{SER} = 0.75H_{In}^{SER} + 0.25H_{Ir}^{SER} \quad (9)$$

where $y_{In}^1 = 1$ denotes the site fraction of Indium in the first sublattice, y_{In}^2 and y_{Ir}^2 the site fractions of indium and iridium in the second sublattice, ${}^{0}G^{In0.75In0.25}$ is the Gibbs energy of the hypothetical compound $In_{0.75}In_{0.25}$.

${}^{xs}G_m^{\lambda}$ is the excess Gibbs energy expressed by the following expression:

$${}^{xs}G_m^{\lambda} = y_{In}^2 y_{Ir}^2 L_{In:In,Ir}^{\lambda} \quad (10)$$

where $L_{In:In,Ir}^{\lambda}$ represents the interaction parameters between the elements In and Ir in the second sublattice while the first sublattice is only occupied by the element In. These excess parameters are temperature dependent as:

$$L_{In:In,Ir}^{\lambda} = a_{\lambda} + b_{\lambda}T \quad (11)$$

In order to avoid the occurrence of the hypothetical compound In_pIn_q or Ir_pIr_q during the phase diagram calculation, the value +5000 J/mol of atoms was added to the functions GHSERIn and GHSERIr, see Tables 2 and 4.

The Gibbs energy function per mole (m) of the formula unit $(In\%,Ir)_{0.6667}(In,Ir\%)_{0.3333}$ is the following:

$$G^{0.6667In0.3333Ir} - H_{0.6667In0.3333Ir}^{SER} = y_{In}^1 y_{Ir}^2\,{}^{0}G^{In::Ir} + y_{Ir}^1 y_{Ir}^2\,{}^{0}G^{Ir:Ir} + y_{Ir}^1 y_{In}^2\,{}^{0}G^{Ir:In} + y_{In}^1 y_{In}^2\,{}^{0}G^{In:In} + RT\left[0.6667\left(y_{In}^1\ln y_{In}^1 + y_{Ir}^1\ln y_{Ir}^1\right) + 0.3333\left(y_{In}^2\ln y_{In}^2 + y_{Ir}^2\ln y_{Ir}^2\right)\right] + {}^{xs}G_m \quad (12)$$

with the same symbols as in [Eq. (8)].

4. Results and discussions

The optimization of the interaction parameters were carried out by taking into account all the relevant experimental data which are detailed in Section 2. But, in order to avoid the occurrence of an unwanted inverted miscibility gap in the liquid phase during the calculation of the phase diagram, additional constraints $\partial^2 G/\partial x^2 > 0$ in the whole Ir composition range (every Δx(Ir) = 0.025) and at different temperatures (every ΔT = 25 K) between 1200 and 4000 K were imposed as previously in other systems [19–21]. The hypothesis of no miscibility gap in the In–Ir system was supported by the reasons argued by [12]. The modelling of the system was performed according to the CALPHAD method [15] with the Thermo-Calc software [22] and the assessment was carried out using the Parrot module [23] of this package.

The optimization was made in several steps.

1. *First* the thermodynamic parameters of the liquid phase were optimized using the numerous and negative integral and scarce partial experimental enthalpies of mixing [11,12]. In the Parrot module, we attributed the weight of 1 to all the experimental data measured up to x(Ir) = 0.35. The other data were discarded because they concerned a two-phase (liquid + compound) domain. Four excess parameters of the Redlich–Kister equation [18] were optimized. The minimum of the curve of the integral enthalpy of mixing of the liquid phase versus the Ir molar fraction was calculated at about −20 kJ/mol and x(Ir) = 0.5. We concluded than no

Table 2
The optimized thermodynamic parameters of the In–Ir system (second optimization, Section 2.2).

Phase	Thermodynamic model	Parameters (units in J/mol atom and J/mol atom K)
Liquid	$(In,Ir)_1$	${}^0L = -78500$ ${}^1L = +16000$ ${}^2L = +22000$ ${}^3L = -11000$
FCC_A1	$(In,Ir)_1\ (Va)_1$	${}^0L^{FCC\_A1}_{In,Ir:Va} = -10000$ ${}^1L^{FCC\_A1}_{In,Ir:Va} = 500$
In_3Ir_LT	$(In)_{0.75}:(In,Ir)_{0.25}$	$G^{In_3Ir\_LT}_{In:In} - H^{Tetragonal\_A6}_{In} = GHSERIn + 5000$ $G^{In_3Ir\_LT}_{In:Ir} - 0.75 * H^{Tetragonal\_A6}_{In} - 0.25 * H^{FCC\_A1}_{Ir} = 0.75 * GHSERIn + 0.25 * GHSERIr - 24900 + 4.378 * T$ ${}^0L^{In_3Ir\_LT}_{In:In,Ir} = -2000$
In_3Ir_HT	$(In)_{0.75}:(In,Ir)_{0.25}$	$G^{In_3Ir\_HT}_{In:In} - H^{Tetragonal\_A6}_{In} = GHSERIn + 5000$ $G^{In_3Ir\_HT}_{In:Ir} - 0.75 * H^{Tetragonal\_A6}_{In} - 0.25 * H^{FCC\_A1}_{Ir} = 0.75 * GHSERIn + 0.25 * GHSERIr - 23800 + 2.645 * T$ ${}^0L^{In_3Ir\_HT}_{In:In,Ir} = -2700$
In_2Ir	$(In,Ir)_{0.6667}:(In,Ir)_{0.3333}$	$G^{In_2Ir}_{In:In} - H^{Tetragonal\_A6}_{In} = GHSERIn + 5000$ $G^{In_2Ir}_{Ir:Ir} - H^{FCC\_A1}_{Ir} = GHSERIr + 5000$ $G^{In_2Ir}_{In:Ir} - 0.6667 * H^{Tetragonal\_A6}_{Ir} - 0.3333 * H^{FCC\_A1}_{Ir} = 0.6667 * GHSERIn + 0.3333 * GHSERIr - 26500 + 1.681 * T$ $G^{In_2Ir}_{Ir:In} - 0.6667 * H^{FCC\_A1}_{Ir} - 0.3333 * H^{Tetragonal\_A6}_{In} = 0.6667 * GHSERIr + 0.3333 * GHSERIn + 10000 + 26500 - 1.681 * T$ ${}^0L^{In_2Ir}_{In:In,Ir} = -14000 + 6 * T$ ${}^0L^{In_2Ir}_{In,Ir:Ir} = +16200 + 1 * T$

(Va) for vacancy.

temperature dependence was necessary as previously indicated by Anres et al. [11].

Fig. 2 shows the very good agreement between the calculated integral enthalpies of mixing of the liquid phase and experimental data of [11,12] up to x(Ir) equal to about 0.35 where only the liquid phase exists. Indeed, when x(Ir) > 0.35 the difference between the calculated integral enthalpies of mixing of the liquid phase and the experimental data of Refs. [11,12] increases. This is due to the precipitation of a solid phase [11,12] revealed by kinks on some experimental curves and then the measured data concern a two-phase domain (liquid + In_3Ir) or (liquid + In_2Ir). The temperatures and compositions of these kinks were identified as liquidus data information by [12].

The four excess parameters of the liquid phase optimized in the present work are similar to the ones by [11] but slightly different because in addition of the data of [11], we took into account the data determined by [12]. Fig. 3 shows the reasonable agreement, within the experimental error bar, between the calculated partial enthalpies of formation of the liquid phase and the experimental data. No temperature dependence is noticed. The calculated limiting partial molar enthalpy of mixing of liquid iridium in liquid indium is equal to −50 kJ/mol.

2. *The second step* of the optimization was relative to the optimization of the enthalpies of formation of the intermetallic compounds. As the experimental data are different from one another, we had to test each one separately. No composition range was first assumed for In_3Ir and In_2Ir. We used the liquidus data

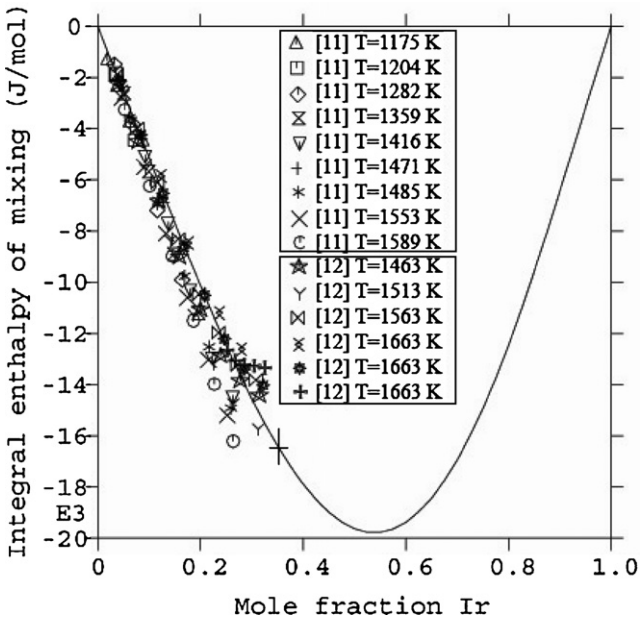

Fig. 2. Calculated and experimental integral molar enthalpies of mixing of the liquid phase. The error bar is ±4% (|) for $\Delta_{mix}H^0_m$ and ±1% (—) for x_{Ir}.

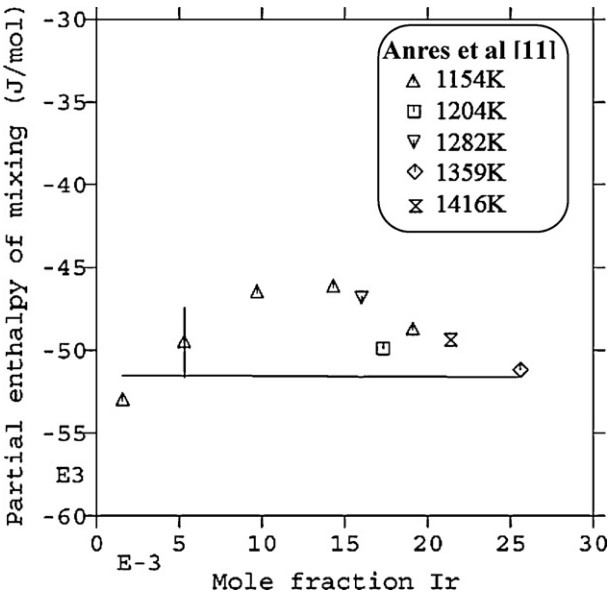

Fig. 3. Calculated and experimental partial enthalpies of mixing of the liquid phase. The error bar on the partial enthalpy of mixing was evaluated at about ±4% by [11].

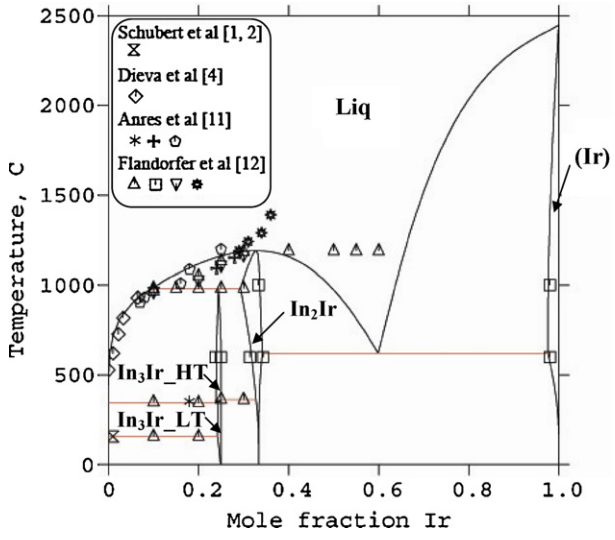

Fig. 4. Comparison of the complete In–Ir phase diagram calculated with the thermodynamic parameters optimized during the second step of the optimization, Table 2, with experimental data.

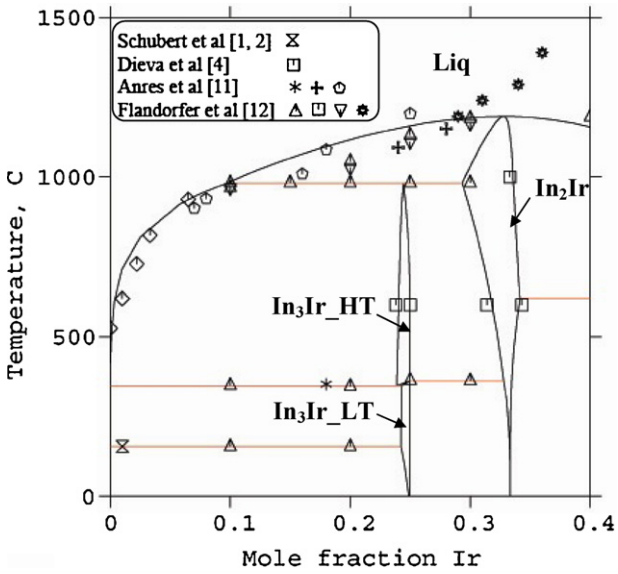

Fig. 5. Comparison of the In–Ir phase diagram in the In rich part (calculated on the basis of the thermodynamic parameters optimized during the second step of the optimization, Table 2) with the experimental data.

[1,2,11,12], the temperature and the Ir composition of the liquid phase involved in the eutectic and peritectic invariant reactions, the experimental enthalpies of formation of In_3Ir and In_2Ir as well as the Cp values determined by Anres et al. [11].

We kept as valuable the values of the excess parameters of the liquid phase optimized in the first step.

4.1. Test of the data of Anres et al. [11]

We first used as initial values (at 298.15 K with the reference state In tetragonal_A6, Ir FCC_A1), the values [a_i, Eq. (7)] of the respective enthalpies of formation (−0.651 and −5.735 kJ/mol) of the two intermetallic compounds recalculated on the basis of the available molar ones of the In_3Ir and In_2Ir compounds (−9 and −14 kJ.mol, extrapolated at T = 1175 K by Anres et al. [11] with the reference state In and Ir liquid at 1175 K). No temperature parameter [b_i, Eq. (7)] was considered. The above enthalpies of formation of the two intermetallic compounds In_3Ir and In_2Ir used to describe the phase diagram are not enough negative to allow their stability at high temperatures, and the liquid was stable down to 0 °C in the central part of the diagram.

Then we used as initial values [a_i, Eq. (7)], the recalculated values at 298.15K (−2.651 and −7.397 kJ/mol) from the higher negative values of the respective enthalpies of formation of the two compounds within the error bar (±2 kJ/mol) indicated by Anres et al. [11], i.e. −11 (In_3Ir) and −16 kJ/mol (In_2Ir), and no temperature dependence [b_i, Eq. (7)] was assumed. Once again, the liquid was stable down to 0 °C in the central part of the diagram. Only one invariant reaction was calculated (Liq ↔ In + In_2Ir). As mentioned above in the paragraph, the enthalpies of formation of In_3Ir and In_2Ir are not yet enough negative to allow their stability at high temperatures.

4.2. Test of the data of Meschel and Kleppa [14]

We used the enthalpy of formation of the In_3Ir_HT compound (−23.8 ± 2.4 kJ/mol, reference states SER at 298.15 K) measured by Meschel and Kleppa [14] and optimized the ones of In_3Ir_LT and In_2Ir. We took into account the small homogeneity range determined by EPMA [12], for the In_3Ir (0.238–0.25 Ir) and In_2Ir (0.314–0.343 Ir) phases. In addition, the experimental structural transformation In_3Ir_LT ↔ In_3Ir_HT at 625 K was assumed. A coher-

Table 3
Invariant reactions in the In–Ir system calculated after the second step of optimization (Section 2.2).

Reactions	T (°C) [Ref.]	Phase x(Ir) [Ref.]	T (°C) Thiswork	Phase x(Ir) This work
Liq ⇔ In + In_3Ir_LT	156 ± 2 [12] 156.64 ± 0.02 [11]	In_3Ir_LT 0.238–0.25 [12]	156.8	Liq 3.41E−08 In 0.0000 In_3Ir_LT 0.2424
In_3Ir_HT ⇔ Liq + In_3Ir_LT	347 ± 3 [12] 352 [11]	In_2Ir 0.314–0.343 [12]	347.0	Liq 3.71E−05 In_3Ir_LT 0.2425 In_3Ir_HT 0.2386
In_2Ir + In_3Ir_HT ⇔ In_3Ir_LT	363 ± 3 [12]		361.7	In_2Ir 0.3278 In_3Ir_HT 0.2500 In_3Ir_LT 0.2500
Liq + In_2Ir ⇔ In_3Ir_HT	981 ± 3 [12] 985 [11]		981	Liq 0.0976 In_2Ir 0.2934 In_3Ir_HT 0.2442
Liq ⇔ In_2Ir			1190	Liq 0.3300 In_2Ir 0.3300
Liq ⇔ In_2Ir + (Ir)	1188 ± 5 [12] 1190 [11]		621.1	Liq 0.5984 In_2Ir 0.3414 (Ir) 0.9752

Table 4
Optimized thermodynamic parameters to reproduce the experimental phase diagram drawn by Flandorfer et al. [12], third optimization.

Phase	Thermodynamic model	Parameters (units in J/mol atom and J/mol atom K)
Liquid	$(In,Ir)_1$	${}^0L = -6500$ ${}^1L = -15000$ ${}^2L = -7000$ ${}^3L = -2000$
FCC_A1	$(In,Ir)_1\ (Va)_1$	${}^0L^{FCC\_A1}_{In,Ir:Va} = 35000 + 8 * T$ ${}^1L^{FCC\_A1}_{In,Ir:Va} = 25000$
In_3Ir_LT	$(In)_{0.75}:(In,Ir)_{0.25}$	$G^{In_3Ir\_LT}_{In:In} - H^{Tetragonal\_A6}_{In} = GHSERIn + 5000$ $G^{In_3Ir\_LT}_{In:Ir} - 0.75 * H^{Tetragonal\_A6}_{In} - 0.25 * H^{FCC\_A1}_{Ir} = 0.75 * GHSERIn + 0.25 * GHSERIr - 24900 + 11.303 * T$ ${}^0L^{In_3Ir\_LT}_{In:In,Ir} = -2500$
In_3Ir_HT	$(In)_{0.75}:(In,Ir)_{0.25}$	$G^{In_3Ir\_HT}_{In:In} - H^{Tetragonal\_A6}_{In} = GHSERIn + 5000$ $G^{In_3Ir\_HT}_{In:Ir} - 0.75 * H^{Tetragonal\_A6}_{In} - 0.25 * H^{FCC\_A1}_{Ir} = 0.75 * GHSERIn + 0.25 * GHSERIr - 23800 + 9.568 * T$ ${}^0L^{In_3Ir\_HT}_{In:In,Ir} = -3000$
In_2Ir	$(In,Ir)_{0.6667}:(In,Ir)_{0.3333}$	$G^{In_2Ir}_{In:In} - H^{Tetragonal\_A6}_{In} = GHSERIn + 5000$ $G^{In_2Ir}_{Ir:Ir} - H^{FCC\_A1}_{Ir} = GHSERIr + 5000$ $G^{In_2Ir}_{In:Ir} - 0.6667 * H^{Tetragonal\_A6}_{In} - 0.3333 * H^{FCC\_A1}_{Ir} = 0.6667 * GHSERIn + 0.3333 * GHSERIr - 26700 + 11.135 * T$ $G^{In_2Ir}_{Ir:In} - 0.6667 * H^{FCC\_A1}_{Ir} - 0.3333 * H^{Tetragonal\_A6}_{In} = 0.6667 * GHSERIr + 0.3333 * GHSERIn + 10000 + 26700 - 11.135 * T$ ${}^0L^{In_2Ir}_{In:In,Ir} = -18700 + 10.8 * T$ ${}^0L^{In_2Ir}_{In,Ir:Ir} = +16200 + 1.0 * T$

(Va) for vacancy.

ent set of optimized parameters was obtained, Table 2. Fig. 4 gives the complete calculated phase diagram compared to the experimental data. The temperature and composition of the eutectic reaction: Liq ↔ In + In_3Ir_LT are well reproduced, Table 3. Its temperature 429.8 K is within the error bar 429 ± 2 K given by Flandorfer et al. [12]. Thus the calculated temperature 1254 K of the peritectic invariant reaction Liq + In_2Ir ↔ In_3Ir_HT is also in good agreement with the experimental 1254 ± 3 K [12] or 1258 K one [11]; the Ir composition of the liquid phase (0.097 Ir) is quite in agreement with the one (0.10 Ir) mentioned in [12], Table 3. In_2Ir shows a congruent melting at 1463 K. The calculated In_2Ir liquidus reproduced the experimental data very well especially in the high Ir part. In the low Ir part, the agreement is somehow less good but taking into account the difference between the results from calorimetric measurements (1200 K) and DTA (1258 K) for the peritectic reaction: Liq + In_2Ir ↔ In_3Ir_HT [12], the composition of liquid participating in the reaction may be somehow uncertain. In fact in the composition range $0.35 \leq x(Ir) \leq 1$, instead of the peritectic reaction Liq + (Ir) ↔ In_2Ir a eutectic reaction (Liq ↔ In_2Ir + (Ir)) was observed at T = 894.1 K for x(Liq,Ir) = 0.598, Fig. 4 and Table 3. The solubility limit (about 0.98 Ir) of the FCC_A1 (Ir) solid solution at T = 850 K and 1250 K [12] is well calculated.

A zoom of Fig. 4 in shown in Fig. 5 in the In rich part. It will be noted that the transformation Liq + In_3Ir_LT ↔ In_3Ir_HT occurs at 620.0 K while the In_2Ir + In_3Ir_HT ↔ In_3Ir_LT reaction takes place at 634.7 K. These results are in good agreement with the experimental data of Flandorfer et al. [12] and his two suggestions of a possibly metatectic transformation at 620 ± 3 K and a peritectoïd one at 636 ± 3 K.

In Fig. 6a and b the molar heat capacities calculated between 300 and 800 K for the In_3Ir_LT and In_2Ir phases are compared at once with the data of Anres et al. [11] and the ones obtained from the Neumann and Kopp rule from the Cp values of pure In and Ir taken from Dinsdale [17]. The agreement is more satisfactory for In_2Ir than for In_3Ir_LT. In order to avoid the anomaly of the heat capacity of In (bump at T = 429.75 K occurring when the GHSERIn Gibbs energy is represented as the power series in terms of temperature described by [17] in the 429.75 K < T < 3800 K range), the power series of the 298.15 K < T < 429.15 K range was used for temperatures higher than 429.75 K.

Table 5
Invariant reactions in the In–Ir system calculated after the third step of optimization (calculation of the interpolated phase diagram by Flandorfer et al. [12]).

Reactions	T (°C) [Ref.]	Phase x(Ir) [Ref.]	T (°C) This work	Phase x(Ir) This work
Liq ⇔ In + In_3Ir_LT	156 ± 2 [12] 156.64 ± 0.02[11]	In_3Ir_LT 0.238-0.25 [12]	156.8	Liq 2.6E−09 In 0.0000 In_3Ir_LT 0.2382
In_3Ir_HT ⇔ Liq + In_3Ir_LT	347 ± 3 [12]	In_2Ir 0.314-0.343 [12]	347.6	Liq 1.8E−05 In_3Ir_LT 0.2400 In_3Ir_HT 0.2366
In_2Ir + In_3Ir_HT ⇔ In_3Ir_LT	363 ± 3 [12]		361.0	In_2Ir 0.3208 In_3Ir_HT 0.2500 In_3Ir_LT 0.2500
Liq + In_2Ir ⇔ In_3Ir_HT	981 ± 3 [12] 985 [11]		981	Liq 0.1012 In_2Ir 0.3080 In_3Ir_HT 0.2452
Liq ⇔ In_2Ir + (Ir)	1188 ± 5 [12] 1190 [11]		1188	Liq 0.3057 In_2Ir 0.3837 (Ir) 0.9621

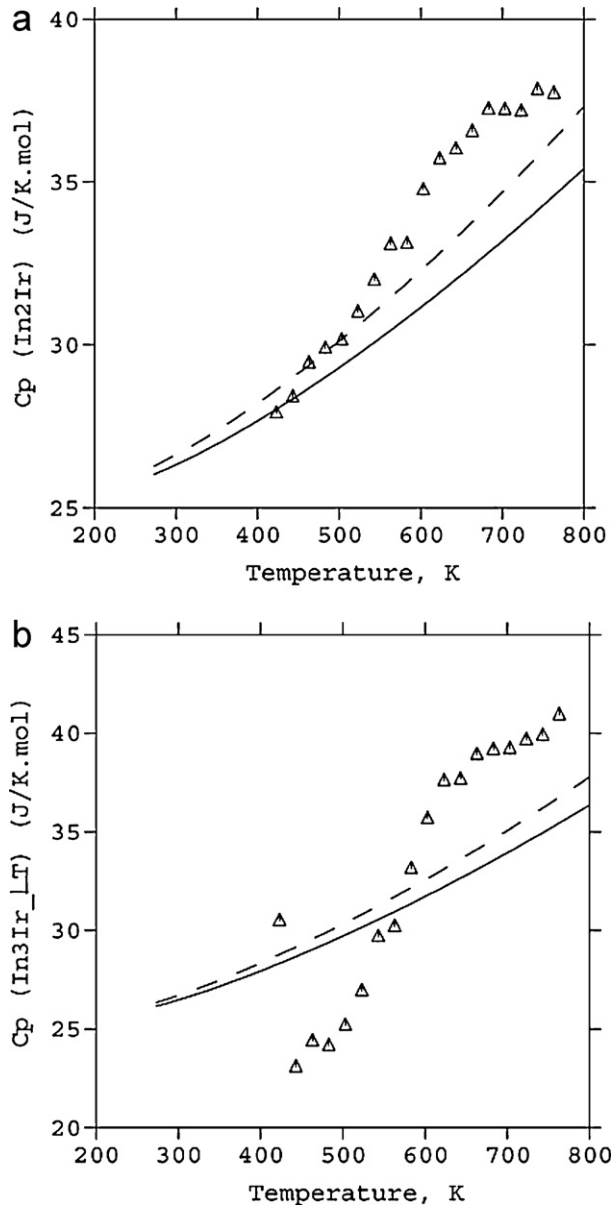

Fig. 6. (a) Molar heat capacities calculated between 300 and 800 K (continuous line) for the In_2Ir phase and compared with the data of Anres et al. [11] (△) and the Neumann and Kopp rule (dashed line). (b) Molar heat capacities calculated between 300 and 800 K (continuous line) for the In_3Ir_LT phase and compared with the data of Anres et al. [11] (△) and the Neumann and Kopp rule (dashed line).

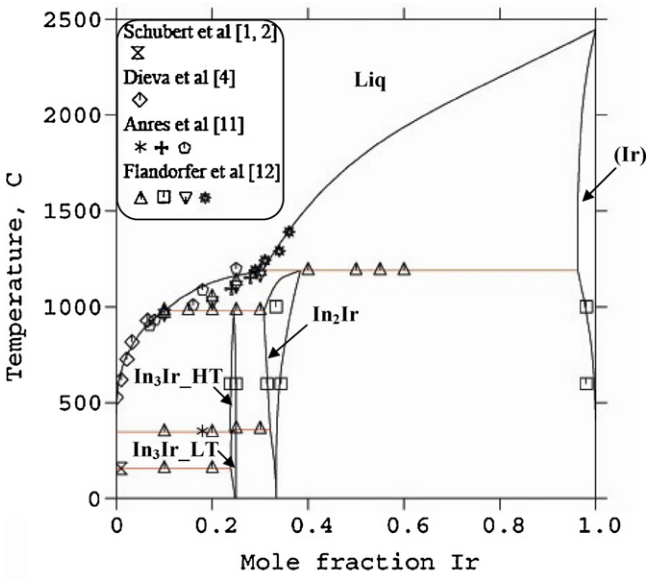

Fig. 7. Comparison of the In–Ir phase diagram calculated with the thermodynamic parameters optimized during the third procedure, Table 4, with the experimental data.

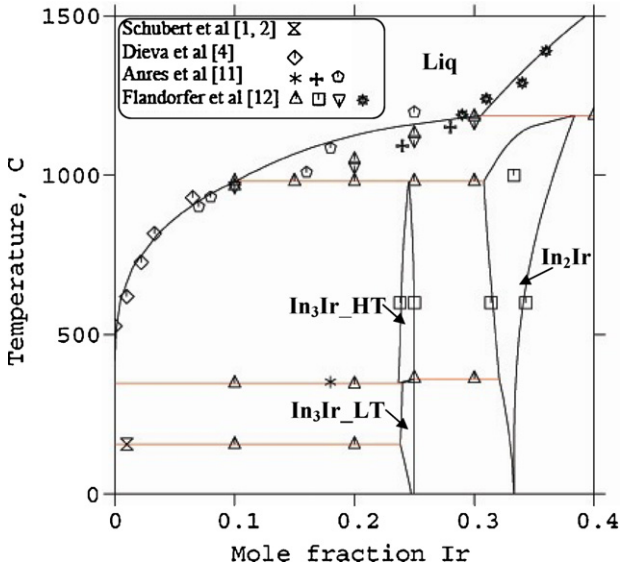

Fig. 8. Part of the In–Ir phase diagram in the In rich part calculated with the thermodynamic parameters optimized during the third procedure, Table 4, and compared with the experimental data.

3. *Finally, in a third optimization step*, we tried to reproduce the liquidus interpolated by Flandorfer et al. [12] in the composition range $0.35 \le x(\mathrm{Ir}) \le 1$ and obtained a second set of optimized thermodynamic parameters.

Compared to the first set, the two negative excess parameters of the liquid phase (^0L and ^3L) were lowered very much (in absolute value) in order to diminish its stability at low temperatures, Table 4. So no agreement could be found with the coherent integral and partial experimental data of enthalpies of mixing of the liquid phase determined by [11,12]. In this last step of the process, a homogeneity range was also assumed for the two intermetallic compounds, Fig. 7. In addition the structural change at about $T = 625$ K (LT ↔ HT) of the In_3Ir phase [11,12] was taken into account, Fig. 8. The eutectic reaction: Liquid ↔ In + In_3Ir_LT, and the two peritectic reactions: Liq + In_2Ir ↔ In_3Ir_HT and Liq + (Ir) ↔ In_2Ir were resulted, Table 5. The calculated peritectic reaction (Liq + (Ir) ↔ In_2Ir) at 1461 K is in agreement with the predicted one (1461 ± 5 K) by [12] or 1463 K [11].

5. Conclusion

A coherent set of thermodynamic parameters was optimized based on the CALPHAD approach, which led to the calculation of a phase diagram which is in good agreement with the experimental part determined up to about $x(\mathrm{Ir}) = 0.35$.

Beyond this value and up to $x(\mathrm{Ir}) \le 1$, no experimental liquidus data has been determined. In this interpolated part of the phase diagram by [12], our optimization led to the calculation of a eutectic reaction Liq ↔ In_2Ir + (Ir) instead of a predicted peritectic one Liq + (Ir) ↔ In_2Ir.

The calculated integral and partial enthalpies of mixing of the liquid phase of the In–Ir system are in good agreement, within the

experimental error, with the numerous and coherent experimental data up to about $x(\mathrm{Ir}) = 0.35$. Beyond this value, the agreement is not satisfactory due to the precipitation of solid phases in the liquid.

The phase diagram proposed by [12] can only be calculated with a new set of optimized excess thermodynamic parameters of the liquid phase but which cannot give account of the reliable integral and partial enthalpies of mixing determined by [11,12].

Consequently, in the $0.35 \leq x(\mathrm{Ir}) \leq 1$ composition range, the In–Ir phase diagram seems to be more complex than the predicted one as attested by the determination of a new phase $In_{54}Ir_{46}$ by [12] which has been first assumed as metastable and further experimental determinations are therefore needed in the Ir rich part of the phase diagram.

References

[1] K. Schubert, H. Breimer, R. Gohle, H.L. Lukas, H.G. Meissner, E. Stolz, Naturwissenschaften 45 (1958) 360.
[2] K. Schubert, H.L. Lukas, H.G. Meitbner, S. Bhan, Z. Metallkd. 50 (1959) 534.
[3] C. Dasarathy, Trans Metall. Soc. AIME 245 (9) (1969) 2015.
[4] E.N. Dieva, in: V.G. Bamburov (Ed.), Physicochemical Studies of Liquid Metals and Alloys, Izd. Ural'sk. Nauch. Tsentra Akad. Nauk. SSSR, Sverdlovsk, 1974, p.V.G. Bamburov.
[5] M. Ellner, S. Bhan, J. Less-Common Met. 79 (1981) P1–P9.
[6] W.G. Moffat, Handbook of Binary Phase Diagrams, Genium Publishing Company, Schenectady, 1987, 11, 81.
[7] T.D. Massalski, H. Okamoto, P.R. Subramanian, L. Kacprzak (Eds.), Binary Alloy Phase Diagrams, ASM International Materials Park, OH, 1990, p. 2249.
[8] H. Okamoto, in: C.E.T. White, H. Okamoto (Eds.), Phase Diagrams of Indium Alloys and their Engineering Applications, ASM International Materials Park, OH, 1992, p. 140;
H. Okamoto, J. Phase Equilib. 4 (2000) 451.
[9] J. Ågren, Curr. Opin. Solid State Mater. Sci. 1 (3) (1996) 355.
[10] R. Pöttgen, R.-D. Hoffmann, G. Kozyba, Z. Anorg. Allg. Chem. 624 (1998) 244.
[11] P. Anres, P. Fossati, K. Richter, M. Gambino, M. Gaune-Escard, J.-P. Bros, J. Alloys Compd. 296 (2000) 119.
[12] H. Flandorfer, K.W. Richter, E. Hayer, H. Ipser, G. Borzone, J.P. Gros, J. Alloys. Compd. 345 (2002) 130.
[13] M.F. Zumdick, A. Gregory, A. Landrum, R. Dronskowski, R.-D. Hoffmann, R. Pöttgen, J. Solid State Chem. 169 (2000) 19–20.
[14] S.V. Meschel, O.J. Kleppa, J. Alloys Compd. 333 (2002) 91.
[15] L. Kaufman, H. Bernstein, Computer Calculations of Phase Diagrams, Academic Press, New York, NY, 1970.
[16] F.R. De Boer, R. Boom, W.C. Mattens, A.R. Miedema, A.K. Niesen, Cohesion in Metals, North-Holland, Amsterdam, 1988.
[17] A.T. Dinsdale, CALPHAD 15 (1991) 317.
[18] O. Redlich, A. Kister, Ind. Eng. Chem. 40 (1948) 345.
[19] R. Arroyave, Z.K. Liu, CALPHAD 28 (2006) 1.
[20] K.C. Kumar, P. Wollants, J. Alloys Compd. 320 (2001) 189.
[21] S.L. Chen, S. Daniel, F. Zhang, Y.A. Chang, W.A. Oates, R. Schmid-Fetzer, J. Phase Equilib. 22 (2001) 373.
[22] B. Sundman, J.-O. Andersson, CALPHAD 9 (1985) 153.
[23] B. Jansson, Thesis, Royal Institute of Technology, Stockholm, 1984.
[24] W.B. Pearson, in: P. Villars, L.D. Calvet (Eds.), Pearson's Handbook of Crystallographic Data for Intermetallic Phases, American Society for Metals, OH, 1985.